OXFORD

Human Molecular Genetics, 2015, Vol. 24, No. 23 6687–6698

doi: 10.1093/hmg/ddv373
Advance Access Publication Date: 11 September 2015
Original Article

ORIGINAL ARTICLE

Molecular analyses of juvenile granulosa cell tumors bearing *AKT1* mutations provide insights into tumor biology and therapeutic leads

Aurélie Auguste[1,2,†], Laurianne Bessière[1,2,†], Anne-Laure Todeschini[1,2,†,*], Sandrine Caburet[1,2], Sabine Sarnacki[3,4], Jaime Prat[5], Emanuela D'angelo[5], Pierre De La Grange[6], Olivier Ariste[6], Fréderic Lemoine[6], Bérangère Legois[1,2], Charles Sultan[7,8], Alain Zider[1,2], Louise Galmiche[3,4], Nicolas Kalfa[7,8] and Reiner A. Veitia[1,2,*]

[1]Institut Jacques Monod, Université Paris Diderot, CNRS UMR7592, Paris 75013, France, [2]Faculty of Biological Sciences, Université Paris Diderot-Paris VII, 75205 Paris, France, [3]Hôpital Necker-Enfants Malades, Paris, France, [4]Faculty of Medicine, Université Paris Descartes-Paris V, 75015 Paris, France, [5]Department of Pathology, Hospital de la Santa Creu i Sant Pau, Autonomous University of Barcelona, Barcelona, Spain, [6]GenoSplice, Ltd, Paris, France, [7]Deparment of Pediatic Endocrinology, University Hospital of Montpellier, Montpellier, France and [8]Deparment of Pediatic Surgery, Hôpital Lapeyronie, CHU Montpellier et Université de Montpellier, Montpellier, France

*To whom correspondence should be addressed. Tel: +33 1 57 27 81 16; Email: veitia.reiner@ijm.univ-paris-diderot.fr (R.A.V.); todeschini@ijm.univ-paris-diderot.fr (A.-L.T.)

Abstract

Juvenile granulosa cell tumors (JGCTs) of the ovary are pediatric neoplasms representing 5% of all granulosa cell tumors (GCTs). Most GCTs are of adult type (AGCTs) and bear a mutation in the *FOXL2* gene. The molecular basis of JGCTs is poorly understood, although mutations in the *GNAS* gene have been reported. We have detected in-frame duplications within the oncogene *AKT1* in >60% of the JGCTs studied. Here, to evaluate the functional impact of these duplications and the existence of potential co-driver alterations, we have sequenced the transcriptome of four JGCTs and compared them with control transcriptomes. A search for gene variants detected only private alterations probably unrelated with tumorigenesis, suggesting that tandem duplications are the best candidates to underlie tumor formation in the absence of *GNAS* alterations. We previously showed that the duplications were specific to JGCTs. However, the screening of eight AGCTs samples without *FOXL2* mutation showed the existence of an *AKT1* duplication in one case, also having a stromal luteoma. The analysis of RNA-Seq data pinpointed a series of differentially expressed genes, involved in cytokine and hormone signaling and cell division-related processes. Further analyses pointed to the existence of a possible dedifferentiation process and suggested that most of the transcriptomic dysregulation might be mediated by a limited set of transcription factors perturbed by AKT1 activation. Finally, we show that commercially available AKT inhibitors can modulate the *in vitro* activity of various mutated forms. These results shed light on the pathogenesis of JGCTs and provide therapeutic leads for a targeted treatment.

[†]Drs Auguste, Bessière and Todeschini contributed equally to this work.

Received: July 24, 2015. **Revised:** September 4, 2015. **Accepted:** September 7, 2015

Introduction

Ovarian tumors are classified into three clinicopathological categories with distinct histopathological features: epithelial, sex cords-stromal and germ cell tumors. Granulosa cell tumors (GCTs) represent 90% of the sex cords-stromal tumors and constitute ~5% of ovarian cancers (1). GCTs are subdivided into two distinct forms, the adult (AGCTs) and the juvenile (JGCTs) forms, representing 95 and 5% of the tumors, respectively. Distinction between JGCT and AGCT is primarily based on clinicopathological characteristics (1,2). JGCTs are rare ovarian neoplasms affecting prepubertal girls and young women with a mean age of onset of around 8 years (3,4). The majority of patients diagnosed with JGCT present with an early-stage disease, with a tumor limited to the ovary and have a good prognosis with a survival rate >90% with surgery alone (5–8). However, patients with advanced-stage disease and widely spread tumors or recurrent cases have a very poor prognosis and are more difficult to treat. Although tumor recurrence is not common, it can occur at any stage. Patients may relapse as late as 48 months after the operation, which requires tumor surveillance (9). Because JGCTs are hormonally active, patients can be diagnosed with precocious pseudopuberty owing to increased estrogen secretion (4,7). In general, patients present with precocious breast development, abdominal swelling, pain and palpable tumors, vaginal bleeding or menstrual irregularities, depending on the patient age. Rare cases of virilization have also been observed (10).

AGCTs are characterized by a somatic mutation affecting the *FOXL2* gene (c.402C→G; p.C134W), which encodes a transcription factor (TF). This mutation has been identified in 97% of the AGCTs studied and is absent from JGCTs and other ovarian neoplasms (11–13). The mutation perturbs transforming growth factor beta (TGF-beta) signaling in granulosa cells (14). Unlike the adult subtype, the molecular basis of JGCTs is less well known. However, it is known that JGCTs exhibit a decreased FOXL2 expression compared with a normal ovary, which correlates with an aggressive pattern of progression (15). Pre-ovulatory growth of the somatic cells of the ovary is induced by the follicle-stimulating hormone (FSH), and alterations in its signaling pathway have been suggested to play a role in tumorigenesis. Consistently, two activating mutations of the stimulatory alpha subunit of a trimeric G protein (Gαs), located at Position 201, have been identified in 30% of a JGCT cohort (16). The Gαs protein carrying these activating mutations is encoded by *GNAS*, also termed the gsp oncogene (17). Specifically, mutations R201C and R201H may inhibit the GTPase activity, maintaining Gαs in its active form leading to cell proliferation and tumoral invasiveness (18,19). Because not only FSH but other mitogens such as insulin-like growth factors (IGFs) also signal through PIK3CA and AKT in ovarian somatic cells (20,21), we hypothesized that alterations in this pathway might be involved in the molecular pathogenesis of JGCTs. Consistently, we were able to detect in-frame tandem duplications within *AKT1* as well as an array of point mutations altering highly conserved residues, in a cohort of 16 JGCTs (22) (Table 1). Interestingly, we also found two co-occurring substitutions Gln79Lys and Trp80Arg mapping immediately after the protein region altered by the insertions. The tandem duplications alter the pleckstrin-homology domain (PHD) of AKT1. The PHD binds to phosphatidylinositol-di/trisphosphates from the plasma membrane, which are produced by activated PI3K (23). This leads to the translocation of AKT to the plasmalemma. In such conditions, several kinases can phosphorylate it, whose full activation is achieved upon phosphorylation of Ser473 (24). The wild-type (WT) AKT1-mCherry fusion protein displayed a rather diffuse localization, whereas the mutated proteins were highly enriched at the membrane. A western blot analysis using an antibody directed against phosphorylated Ser473 showed a dramatic phosphorylation difference between the WT and the mutated proteins (25,26). FOXO factors are negatively regulated by AKT in response to a series of growth factors and other signals. Phosphorylation of the FOXOs by AKT causes their sequestration in the cytoplasm, thus preventing transactivation of their targets (27). These factors function as a trigger for apoptosis and protect the cell from oxidative stress by upregulating antioxidants agents such as catalase and superoxide dismutase (27). Using a FOXO3a-based reporter system, we showed that WT AKT1 elicited the expected response: in the presence of serum (i.e. growth factors), FOXO3a was repressed, whereas in serum-starved cells, it repressed FOXO3a less strongly. On the contrary, mutated AKT1 proteins were hyperactive and insensitive to serum deprivation leading to permanent FOXO repression.

Table 1. Clinical and mutation data of the JGCT patients

Patient/ tumor no.	Age (years)	Estradiol (pg/ml)	Testosterone (ng/ml)	*AKT1* exon 3 duplication length (bp)
1	6y	NA	NA	36
2	4y3/12	44	NA	–
3	4y2/12	19	0.19	30
4	13y5/12	320	0.2	–
5	6y	17	1.1	36
6	13y1/12	High	Normal	–
7	14y6/12	23	3.69	–
8	6y9/12	157	2.4	36
9	Neonatal	760	1.1	–
10	1y	10	NA	–
11	1y5/12	<3	<0.07	39
12	10y8/12	18	0.10	48
13	8y6/12	100	<0.07	48
14	7y10/12	103	0.82	36
15	2y2/12	1116	2.2	24
16	0y9/12	NA	NA	36

NA: not available. Table modified from (22).

In the present study, we have performed a mutational analysis of four tumors bearing AKT1 insertions using RNA-Seq data. We found that the in-frame duplications were the sole detectable lesions that were common to the four tumors. This analysis points to the AKT1 mutations as the most obvious alterations in these tumors. We have also uncovered interesting transcriptomic signatures of these tumors. Finally, we have tested the effect of several AKT inhibitors that proved to be active on the mutated proteins holding promise for treating this pediatric tumor.

Results and Discussion

Transcriptome-wide mutational exploration of JGCTs

We have previously proposed that the mutations that we have found in AKT1 are major drivers of tumorigenesis. However, in many instances, tumorigenesis relies on a series of mutational steps altering several genes. That is why we set up to sequence the transcriptome of four JGCT samples (T13–T16), which were all positive for the duplications within the *AKT1* gene. The mutations in the relevant tumors were T13: c.181_228dup, p.(Gln61_Arg76dup); T14: c.202_237dup, p.(Pro68_Gln79dup); T15: c.207_230dup, p.(Arg76_Cys77insTrpProAsnThrPheIleIleArg) and

T16: c.197_232dup, p.(Cys77_Leu78insGlnArgProArgProAsnThr PheIleIleArgCys).

RNA-Seq data were analyzed as described in more detail in the Supplementary Material. For variant filtering, we concentrated on non-synonymous SNPs and small indels (see considerations on coverage and variant allele frequencies/VAF below). Since the matching somatic tissue was not available, we removed the variants present in at least one control sample and those detected by the 1000G project or present as common variants in dbSNP or the Exome Aggregation Consortium (ExAC) database. However, we kept reported pathogenic variants. Next, we focused on the candidate variants predicted as deleterious by SIFT (http://sift.jcvi.org/) and/or possibly/probably damaging by PolyPhen (http://genetics.bwh.harvard.edu/pph2/). We manually checked the quality of the mapping of the reads involving the candidate variants using the Integrative Genome Viewer (IGV) (28). To avoid missing alterations in poorly expressed genes, we retained for confirmation variant candidates supported by as low as two IGV-verified reads. We considered substitutions with apparent VAF >5% (note we are working with cDNA) even if our focus was mutational events responsible for early steps of tumorigenesis (expected VAFs >>5%) and not arising late during this process. Using Blast, we ruled out a few candidates mismapped on paralogous sequences. At this point, 123 candidates remained (out of the initial 3745) to be tested by either Sanger sequencing or polymerase chain reaction (PCR) amplification and digestion with restriction enzymes differentially cutting the WT and the mutated fragments (i.e. PCR-restriction-fragment length polymorphism analysis or PCR-RFLP).

For each gene harboring a candidate variant, the relevant region around it was amplified by PCR from gDNA of T13–T16. First, we focused on variants present in more than one tumor and on genes having at least two variants in order to find common variants potentially underlying JGCTs along with the *AKT1* in-frame duplications. We found 11 candidate variants meeting these criteria (in genes: *NEPPS*, *PPP6R1*, *TET1*, *AREL1*, *MLH1*, *POLR2E*, *ADAMTS12*, *RNF208*, *ACSS1*, *NAP1L4* and *NCAPG2*). However, they could not be confirmed by Sanger sequencing. As shown in the Supplementary Material, Table S3, neither low coverage nor low VAF can explain this result and we conclude to artifactual next generation sequencing calls in most instances.

Then, we focused on variants specific to one tumor, to be subsequently studied in the rest of the cohort (T1–T12). At this point, we had 32, 32, 35 and 22 candidate variants in T13, 14, 15 and 16, respectively. The Sanger sequencing or PCR-RFLP allowed the confirmation of 22, 18, 18 and 10 variants in the respective tumors (Table 2). The inspection of the list of mutated genes along with an enrichment analysis (performed with Enrichr) shows the presence of mutated genes involved cell cycle control, phosphatidylinositol, NOTCH and TGF-beta signaling and other potentially interesting pathways. However, the *P*-values did not withstand a correction for multiple comparisons. The presence/absence of 21 of these mutations in the formalin-fixed paraffin-embedded (FFPE) samples (T1–T12) was assessed by PCR-RFLP. This RFLP survey showed that all of the mutations were private variants (i.e. absent from T1 to 12) whose link with tumorigenesis cannot be formally established because they may simply reflect the genetic load of the patients. This mutation analysis lends credence to our previous idea that the tandem duplications within AKT1 are the best common candidates to underlie tumorigenesis in the tumors studied, which lack the previously reported mutations in *GNAS*.

In our previous work, we screened by PCR the gDNA of AGCTs positive for the *FOXL2* mutation (29), colorectal carcinoma samples (13) and the NCI cell lines and found no evidence for the existence of *AKT1* in-frame duplications in such samples. In order to further explore the specificity of these mutations, we analyzed eight samples of AGCTs negative for the oncogenic *FOXL2* mutation and found the *AKT1* insertion in one of the tested DNAs. The Sanger sequencing of the isolated DNA bands showed that the mutation corresponded to the in-frame duplication c.202_237dup, leading at the protein level to a duplication of the sequence PRPNTFIIRCLQ (p.(Pro68_Gln79dup)) that we had previously observed in T14 (Fig. 1). A reexamination of this tumor in the light of this finding confirmed its classification as an AGCT. However, of note, this patient also had a stromal luteoma in the contralateral ovary. Interestingly, whereas AGCT lacks luteinization (except in pregnancy), JGCTs typically show luteinization of both granulosa and theca cells. The presence of this mutation in an AGCT with WT *FOXL2* and a stromal luteoma component suggest that GCTs may be a continuum ranging from typical AGCTs to typical JGCTs but including a twilight zone of AGCTs without the *FOXL2* mutation but bearing *AKT1* mutations and JGCTs with WT *AKT1* and mutated *GNAS*.

Transcriptomic analysis of AKT1-mutated JGCTs

We took advantage of the RNA-Seq data to explore the transcriptomic differences between the tumors and normal samples. This analysis pinpointed 460 differentially expressed genes (DE genes, 136 genes upregulated in the tumors and 324 down-regulated compared with the control samples). A gene set enrichment analysis using Enrichr showed that these 460 DE genes were involved in biological processes such as cytokine-mediated signaling, response to hormones including steroids and gonadotropins and cell division-related processes. Indeed, the 136 genes up-regulated in JGCTs were significantly enriched in genes involved in the regulation of mitosis and chromosome segregation, such as *TOP2A*, *NUSAP1*, *KIF11*, *BUB1*, *CENPE* and *CENPF*. This is rather expected and consistent with the neoplastic nature of JGCTs. With regard to signaling, growth factor and cytokine activities, genes such as those encoding interferons A2 (IFNA2) and A13 (IFNA13), GDF3, GDF7, INHBB, GREM1, TNFSF4 and CSPG5 were upregulated, whereas *CCL3*, *CCL2*, *LIF*, *GDF9*, *AREG*, *EREG*, *TNF*, *IL6*, *TNFSF11*, *LEFTY2*, *DKK1*, *GDF9*, *FGF12* and *HBEGF* were underexpressed in the tumors. Interestingly, the up-regulated genes also displayed an interferon (IFN) signature (*MX1*, *HLA-B*, *HLA-A*, *ADAMTS12*, *IFIT1*, *HERC5*, *IFI27*, *OAS1*, *OAS2*, *OAS3*, *TFF2*, *NCAM1*, *XAF1*, *HLA-DQB1*). This may point toward an auto/paracrine activation of the IFN pathway (30), the relevance of which is to be studied. In this context, it is worth noting that activation of the AKT pathway by the IFN receptors complements the function of IFN-activated janus kinase and signal transducer and activator of transcription (JAK-STAT) pathway, by allowing/enhancing translation of IFN-stimulated genes (ISGs) (31). Interestingly, increased expression of ISGs has been identified in cancer cells compared with corresponding normal cells with correlations to the degree of tumor invasion. Moreover, expression of some IFN-induced genes has been shown to be higher in metastatic cancer than in non-metastatic cells. Finally, the depletion of IRF2, a repressor of IFN-α/β expression, significantly increases tumor growth by increasing proliferation and decreasing apoptosis in tumor models (32). The signature of an immune response also appears in a mouse model of GCT depleted for Foxo1/3 and Pten (33). Such a response seems to be specific because it is not observed in GCTs that develop in the *Ctnnb/Pten*, *Ctnnb1/Kras* or *Smad1/5* mutant mice (33). We have previously studied the transcriptomic profile of AGCTs and have not noticed such a response either (29).

Table 2. Mutations confirmed by Sanger sequencing (and by restriction enzyme digestion, when indicated)

Gene	Mutation (nucleic acid)	Mutation (protein)	Tumor	RFLP-enzyme	Coverage (reads)	VAF %	ExAC allele frequency
ACPL2	NM_001037172.2:c.163C>A	p.P55T	T14	–	11	54.6	–
AEBP1	NM_001129.4:c.803G>A	p.R268Q	T13	–	253	40.3	0.00002197
ALKBH1	NM_006020.2:c.872G > A	p.R291H	T13	–	46	45.7	–
AMOTL1	NM_130847.2:c.1297G > C	p.D433H	T14	NlaIII created	22	31.8	–
ANAPC7	NM_001137664.1:c.1111A > G	p.N371D	T13	–	79	58.2	0.000008590
ANK2	NM_001148.4:c.4496C > T	p.A1499V	T15	–	6	33.3	–
ASXL2	NM_018263.4:c.4207C > T	p.R1403C	T14	BbvI created	14	35.7	0.00001656
BCKDK	NM_001122957.2:c.82C > T	p.R28W	T13	–	37	51.3	–
CDC6	NM_001254.3:c.1469G > A	p.S490N	T16	–	23	56.5	–
CEP350	NM_014810.4:c.2734G > C	p.G912R	T14	MnlI created	8	25.0	–
CPZ	NM_003652.3:c.952A > G	p.T318A	T16	–	97	57.7	AA
CRAMPL1	NM_020825.3:c.3301A > G	p.I1101V	T14	–	16	56.2	–
CUL7	NM_001168370.1:c.205G > A	p.G69S	T13	–	25	52.0	–
DGKD	NM_152879.2:c.398A > G	p.E133G	T15	–	3	66.7	0.000008237
EDEM2	NM_001145025.1:c.473T > A	p.I158N	T15	–	37	32.4	–
ERC1	NM_178039.3:c.2990T > C	p.L997S	T16	–	54	9.3	–
FAM13B	NM_016603.2:c.2510G > A	p.R837Q	T15	XhoI deleted	44	40.9	0.00001666
FEZ2	NM_001042548.1:c.530C > T	p.P177L	T16	MspI deleted	95	33.7	–
GAS6	NM_000820.3:c.928C > A	p.R310S	T13	–	31	38.7	–
HERC4	NM_001278185.1:c.313G > A	p.V105M	T14	–	19	57.9	–
HNRNPUL1	NM_007040.4:c.172G > T	p.G58W	T14	SmaI deleted	61	50.8	–
HR	NM_005144.4:c.2240G > A	p.R747H	T13	–	5	40.0	0.001105
HRNR	NM_001009931.2:c.1991G > A	p.R664Q	T15	–	4	75.0	–
ITPR1	NM_001168272.1:c.2305C > T	p.R769C	T14	–	164	39.0	0.00001657
KPNA1	NM_002264.3:c.23A > G	p.N8S	T15	–	32	28.1	–
LAMA5	NM_005560.4:c.5698G > A	p.V1900M	T14	–	10	100.0	
LAMA5	NM_005560.4:c.9235C > T	p.R3079W	T14	–	11	100.0	
LRRC8B	NM_001134476.1:c.2393C > T	p.T798M	T15	–	19	31.6	0.00004122
LRRFIP2	NM_001134369.2:c.56C > T	p.A19V	T13	PstI deleted	48	39.6	–
LTBP1	NM_000627.3:c.1987C > T	p.R663C	T13	KpnI deleted	45	53.3	–
LTBP3	NM_001130144.2:c.1108T > G	p.C370G	T14	HaeIII created	41	24.4	–
LZTR1	NM_006767.3:c.1889G > A	p.R630Q	T16	BbvI created	18	16.7	0.000008346
MAD1L1	NM_001013836.1:c.851A > G	p.E284G	T14	–	9	44.4	0.000008281
MAP4K3	NM_001270425.1:c.1322G > C	p.C441S	T13	BglII created	72	61.1	–
MICAL1	NM_001159291.1:c.169T > C	p.Y57H	T15	–	16	25.0	0.00001651
MKI67	NM_001145966.1:c.3128A > T	p.E1043V	T16	–	17	35.3	AA
MSL1	NM_001012241.1:c.293A > G	p.H98R	T15	–	384	42.5	–
NOTCH1	NM_017617.3:c.5492T > C	p.L1831P	T13	–	10	40.0	–
NUDT19	NM_001105570.1:c.600G > A	p.W200*	T15	HinfI created	12	41.7	0.00004085
OBSCN	NM_001271223.2:c.26091C > G	p.H8697Q	T14	–	5	80.0	–
OGFOD2	NM_024623.2:c.470A > G	p.H157R	T15	TauI created	20	65.0	–
OTUD4	NM_001102653.1:c.1512G > C	p.L505F	T13	–	10	80.0	–
PLAA	NM_001031689.2:c.1994A > G	p.N665S	T16	–	21	38.1	–
PLAT	NM_000930.3:c.1498G > A	p.G500R	T16	–	85	36.5	0.00008254
PPRC1	NM_001288727.1:c.892G > A	p.G298S	T15	PvuII deleted	30	30.0	0.000008239
PRPF40B	NM_001031698.2:c.1631C > G	p.A544G	T13	–	9	44.4	–
PTPRC	NM_001267798.1:c.3368C > G	p.T1121R	T15	BsaJI created	26	53.9	–
RBFA	NM_001171967.1:c.340A > G	p.S114G	T14	–	79	40.5	0.00004120
REV3L	NM_002912.4:c.3112T > C	p.Y1038H	T16	FokI created	32	40.6	0.000008246
RNF169	NM_001098638.1:c.832T > G	p.F278V	T14	–	8	37.5	–
RNF213	NM_001256071.2:c.8833C > T	p.R2945C	T13	HaeII deleted	42	33.3	0.0005815
RPN2	NM_001135771.1:c.1216C > T	p.L406F	T15	MlyI deleted	258	40.7	–
SH3RF1	NM_020870.3:c.1430G > A	p.R477H	T14	TspRI created	13	38.5	0.000008240
SLK	NM_014720.3:c.3404A > T	p.Q1135L	T14	–	43	51.2	–
SNX25	NM_031953.2:c.1826A > G	p.E609G	T13	–	11	36.4	0.000008242
SPARCL1	NM_001128310.2:c.971C > T	p.P324L	T13	NlaIV deleted	529	40.6	0.000008237
SPHKAP	NM_001142644.1:c.1921G > A	p.D641N	T15	HinfI deleted	54	35.2	–
SPTBN1	NM_003128.2:c.6644A > G	p.K2215R	T16	–	28	46.4	0.000008306
TMEM123	NM_052932.2:c.70G > C	p.G24R	T15	–	105	30.5	0.0001485
TRAPPC9	NM_001160372.2:c.1603A > T	p.T535S	T13	–	31	22.6	AA
TSPYL5	NM_033512.2:c.1127A > G	p.N376S	T13	BseNI created	36	47.2	0.00001647
TTC38	NM_017931.2:c.694G > T	p.D232Y	T13	–	31	29.0	AA

Table continued

Table 2. Continued

Gene	Mutation (nucleic acid)	Mutation (protein)	Tumor	RFLP-enzyme	Coverage (reads)	VAF %	ExAC allele frequency
TTN	NM_133437.4:c.71584A > G	p.I23862V	T15	–	6	50.0	NA
ZNF343	NM_001282495.1:c.1114C > T	p.Q372*	T13	BfaI created	12	33.3	–
ZNF451	NM_001031623.2:c.1203T > G	p.Y401*	T13	BfaI created	20	35.0	–
ZNF512B	NM_020713.2:c.1989C > A	p.D663E	T15	–	6	50.0	–
ZNF548	NM_001172773.1:c.356C > T	p.P119L	T14	–	11	36.4	–
ZNF609	NM_015042.1:c.2807A > C	p.E936A	T13	–	82	25.6	–

AA: ambiguous attribution. ExAC's reference amino acid does not correspond to ours, probably due to the use of different reference transcripts. NA: not available. ExAC: available at http://exac.broadinstitute.org. Since we work with cDNA and not with gDNA, the apparent VAF may be influenced by an allelic expression bias.

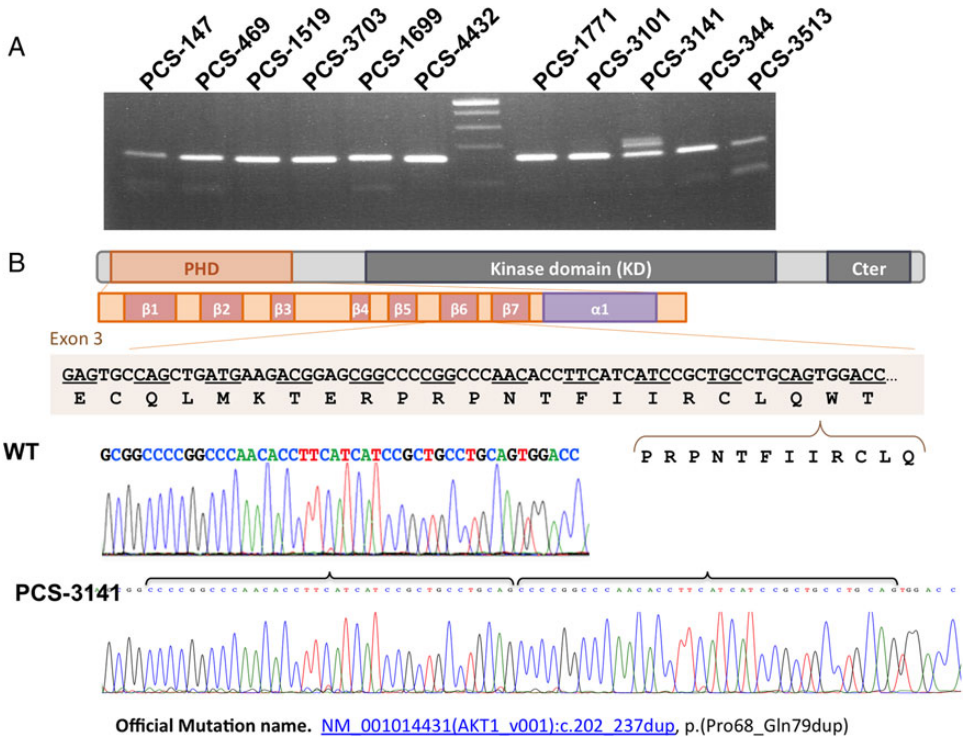

Figure 1. The presence of an AKT1 insertion in an AGCT negative for the oncogenic FOXL2 mutation. (**A**) Agarose gel showing the migration of the amplicons of exon 3 of *AKT1* from gDNA of JGCTs (PCS-147, PCS-469, PCS-1519, PCS-3703, PCS-1699, PCS-4432) and from AGCTs without the FOXL2-C134W mutation (PCS-1771, PCS-3101, PCS-344 and PCS-3513). PCS-3141 is considered as an AGCT on histological grounds. However, the presence of multiple bands on gel lead suggests the existence of an insertion. (**B**) Simplified representation of the AKT1 protein and of the PHD with its secondary structural features (beta strands from 1 to 7 and the C-terminal helix, according to crystallographic data from the Protein Data Bank/PDB Structure 1H10) and the electropherogram of the Sanger sequencing of the exon 3 amplicons from gDNA of a WT sample and the tumor PCS-3141. The tandemly duplicated sequences are highlighted by horizontal brackets pointing to the position of the insertion in the WT sequence. We provide the official name (according to https://www.mutalyzer.nl/name-checker) of the mutation below the electropherogram.

The production of several hormones within the tumors was obviously perturbed. For instance, we detected a 24-fold increase in INHBB mRNA in the tumors. Surprisingly, the levels of *CYP19A1* mRNA, encoding the aromatase, were 22× lower in the tumors than in the normal samples. As previously described, serum levels of estradiol, the product of the aromatase reaction, tended to be elevated in these patients (22) and might reflect tumor size and not aromatase activity per cell. We also found a strong upregulation of the androgen receptor (AR). As expected, DE genes were also characterized by keywords such as ovulation and regulation of reproductive process (Supplementary Material, Table S1).

Among the DE genes in JGCTs, several encoded TFs. Most of them were down-regulated such as *KLF* family members, *GATA6*, *JUNB*, *ATF3*, *SOX9*, *GLIS3*, *NFATC2*, *RORA*, *BACH2*, *NR4A2*, *FOSL1*, *RARB*, *MXD1*, *NKX3-1*, etc. *AR* and *BCL11A* were the most outstanding up-regulated ones. To better pinpoint the possible sources of the dysregulation of the 460 DE genes, we explored whether their *cis* regulatory sequences were targets of TFs compiled in the ChEA database interrogated with EnrichR (ChIP-seq experiments not necessarily performed in ovarian tissue/cells). A total of 155 TFs had ChIP peaks significantly over-represented in the promoters of the 460 DE genes. We refined this list by focusing on the TFs expressed in the ovary and sharing a significant set of target genes with at least another TF. This was assessed on the basis of a significant Pearson's correlation between vectors capturing the absence (0) or the presence (1) of a ChIP peak for the relevant TFs across the DE genes. In order to uncover DE genes potentially co-regulated by the same factors, we retained only those genes sharing a significant set of bound TFs with at least another gene (see details in the Materials and Methods section). This selection led to a list of 332 DE genes bound by 105 'ChIP-TFs'.

A two-way hierarchical clustering of this matrix highlighted three main groups of DE genes (Fig. 2A). The first one involved targets of factors belonging to the polycomb repressing complex PRC2 (EED, PHC1, EZH2, SUZ12). These PRC2 components were grouped with JARID2, RNF2, MTF2 and TP53, which are co-factors of PRC2 (34) (Fig. 2B). The cluster of potential targets contained 66 genes involved in the regulation of stem cell proliferation, cell fate determination and in the response to gonadotropins. Most of the DE genes (three-fourths) were down-regulated in the JGCTs suggesting a possible ongoing dedifferentiation process.

The second cluster of 77 genes comprised known targets of SOX2, POU5F1, NANOG, MYC, EP300, KDM5B, ASH2L, CREM and CREB, many of which belong to a pluripotency network, which represses genes related to differentiation. One-third of the DE genes in this second group were up-regulated in JGCTs, some of which are involved in the regulation of the cell cycle and chromosome segregation such as *TOP2A*, *NUSAP1*, *BUB1* and *KIF11*. The remaining, down-regulated, genes are involved in the differentiation process of various cell types, further supporting the possible dedifferentiation of JGCTs hypothesized above.

Finally, the third group is potentially regulated by a loose group of TFs involving TAL1, FLI1, RUNX1, GATA2, STAT3, AR, SMAD4, YAP1, TCF4, ZNF217, SMARCA4, NR3C1, PPARD, TCF7L2, HNF4A, TCF7, MITF and CDX2. These factors involve nuclear receptors, proteins implicated in stem cell maintenance and Wnt signaling effectors. This less well-defined group of potential targets comprised 89 DE genes, whose distinctive characteristic is that they are not bound by the TFs involved in the previous clusters. The upregulated ones (one-third) were enriched in genes involved in IFN signaling, whereas the down-regulated ones (including the *COX2/PTGS2*) were characterized by the keywords 'inflammatory response' and 'cytokine production'. The latter finding suggests the existence of an anti-inflammatory condition within the JGCTs compared with normal samples, but it may simply reflect a tissue difference if we take into account that ovulation in the normal ovary bears the landmarks of inflammation. Given that the group of TFs defining this cluster recognized many of the 332 DE genes analyzed, we cannot rule out that the formers interact with open chromatin through specific but non-functional binding (i.e. not necessarily meaning regulatory events). Indeed, several genome-wide studies have shown that there is a high degree of overlap in the genomic regions recognized by functionally unrelated TFs (see (35) and references therein). For instance, data on 21 *Drosophila* TFs, with DNA-binding domains belonging to 11 different families, show that about 90% of the 300 most highly bound regions lying within open chromatin are occupied with high confidence by eight or more TFs (36).

The 460 DE genes were also strongly enriched in genes whose expression changes in mouse or cellular models of loss or gain of function for specific TFs (logof-TFs). Namely, 367 DE genes were significant direct or indirect targets of 45 logof-TFs (Fig. 3 and Supplementary Material, Table S1). Most interestingly, these 45 TFs were strongly enriched in phosphorylation targets of AKT1 and of its direct target the GSK3β kinase (Fig. 2B). Of these 45 TFs, 21 belonged to the set of 105 'ChIP-TFs', suggesting that they can be involved in co-regulatory events mediated by the various 'TF complexes' mentioned above. These findings suggest that most of the transcriptomic dysregulation in response to the activation of AKT1 in the JGCTs may be mediated by a limited set of TFs even if their expression levels at the mRNA level do not change (Fig. 3).

It has been suggested that the GCTs in the *Foxo1/3/Pten* mutant mice exhibit features similar to human AGCTs and KGN cells rather than to the JGCTs and COV434 cells (33). This idea is based on the expression profiles of several genes that are similarly altered in the *Foxo1/3/Pten*-depleted GCTs, AGCTs and KGN cells compared with COV434 cells. For instance, *Amh* and *Emx2* were down-regulated, whereas *Foxl2*, *Gata4*, *Smad3*, *Inhbb* and *Sox9* were expressed. We have further tested this idea using the available transcriptomic data for AGCTs (29) and for the Foxo1/3Pten mouse model along with the matching WT granulosa cells. First, we explored the transcriptional changes in the Foxo1/3Pten depleted ovary. To ensure a good reliability of the DE genes obtained, we calculated the average expression levels for all the genes and focused on those whose expression displayed a 2-fold change or more. This allowed us to obtain a list of 3350 genes. With regard to the AGCTs, we used the list of DE genes from our previous work (Online Supplement of (29)). Next, we estimated the statistical significance of the intersection of these lists among themselves and with our list of 460 DE genes (present study). Only the intersection (117 genes) between the latter and the DE genes in the Foxo1/3Pten mouse model was statistically significant. This common gene list is characterized by keywords related to growth factor and cytokine activity and binding. This result suggests that, despite the apparent similarity between the tumors of the Foxo1/3Pten mouse model and AGCTs, the former are closer to JGCTs carrying the *AKT1* insertions studied here. This is not surprising if we consider that hyperactive AKT1 owing to a mutation or to the inactivation of PTEN lead to nuclear exclusion of FOXO factors.

Effect of AKT1 inhibitors on the activity of the mutated forms in JGCTs

Several inhibitors of the PI3K-AKT-mTOR pathway are being tested in clinical trials (37), but it has been described that some AKT1-mutated forms can be resistant to them (38). In order to explore whether commercially available AKT inhibitors were active on the mutated proteins we found in JGCTs, we decided to test their effects using a FOXO3a-based system that we have previously described (22). This reporter system is based on the fact that FOXO factors are negatively regulated by AKT in response to a series of growth factors and other signals. Phosphorylation of the FOXOs at three conserved sites by AKT causes their sequestration in the cytoplasm, preventing transactivation of their targets (27). In the presence of inhibitors, AKT1 phosphorylates its targets less efficiently, and we expect to observe a higher FOXO3a/luciferase activity. Luciferase experiments were performed in HeLa cells co-transfected with the 2X-DBE-luc reporter (containing two binding sites for FOXO3a), a FOXO3a expression vector or a control vector (NLS-mCherry, driving the expression of mChery fused to a nuclear localization signal) and various constructs driving the expression of WT or mutated AKT1 forms.

Five different AKT inhibitors (MK-2206 2HCl, AZD5363, Ipatasertib, A-674563 and GSK690693) were tested, and the results are displayed in Figures 4 and 5. As previously described, WT AKT1 elicited the expected response: in the presence of serum phosphorylated AKT1 repressed FOXO3a (22). The presence of 4 μM of Ipatasertib (Fig. 4A) had almost no impact on WT- and T12-AKT1 activities, but it was able to efficiently repress T16. To further study the differential behavior of Ipatasertib on the various AKT1 forms, we tested the effect of this inhibitor on several other insertion variants. Another mutant (over five tested) was also inhibited by Ipatasertib. The basis of the differential inhibition of these two AKT1 forms by Ipatasertib requires further studies as they differ by the length of the duplicated segment and by the site of insertion. Eight micromolar of AZD5363 had no impact either on WT- or on T12-AKT1 (Fig. 4B), whereas 6 μM of MK-2206

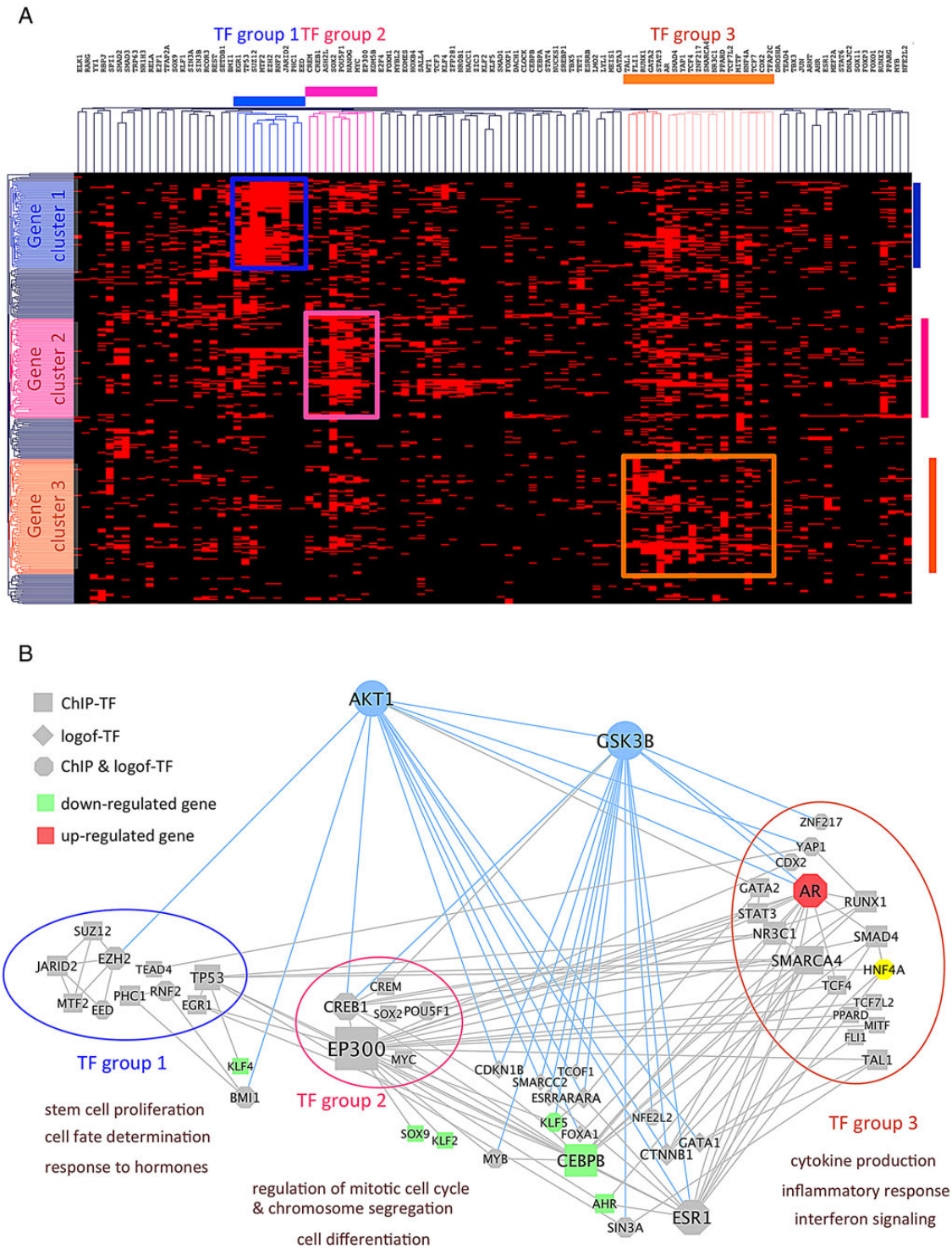

Figure 2. Enrichment of the differentially expressed genes in JGCTs in direct and indirect targets of AKT1. (**A**) Heat map displaying a two-way hierarchical clustering of 105 TFs having ChIP peaks over-represented in the promoters of 332 DE genes. Details of the selection process of both TFs and DE genes involved in the analysis are described the Materials and Methods section. Three main groups of DE genes (and TFs) are highlighted. The first one (in blue) involved 66 genes that are known targets of factors belonging to the polycomb repressing complex PRC2 (EED, PHC1, EZH2, SUZ12) along with some co-factors of PRC2. The second cluster of 77 genes (in magenta) comprises known targets of SOX2, POU5F1, NANOG, MYC, EP300, KDM5B, ASH2L, CREM and CREB, many of which belong to a pluripotency network. The third group (in orange) is potentially regulated by a loose group around RUNX1, GATA2 and AR. (**B**) Signaling network highlighting the enrichment in phosphorylation targets of AKT1 and GSK3B (blue edges) among the possible regulators identified above, namely the ChIP-TF (squares), logof-TF (diamonds) or factors that belong to both sets (octagons). The factors are grouped according to the clustering shown in (A). Some of the factors are also differentially expressed in JGCTs, either down-regulated (in green) or up-regulated (in red). The gene ontology keywords identified for the three groups of DE genes are shown below their respective potential regulators.

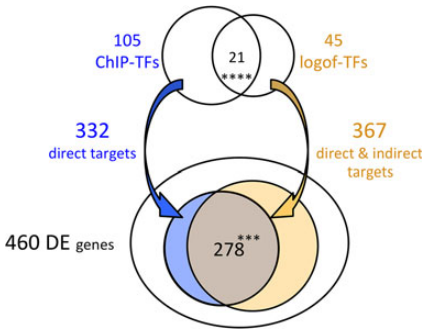

Figure 3. The Venn diagram of the different gene sets identified in the transcriptomic analysis of JGCTs compared with normal controls. The gene set enrichment was performed using Enrichr. The DE genes are strongly enriched in direct targets of 105 TFs, as determined by ChIP experiments in various tissues and cell types (332 of the 460 DE genes). A large part of the 460 DE genes are also direct or indirect targets of 45 TFs, for which loss or gain of function studied are available (367 of the 460 DE genes). Statistical significance of the overlaps: ***$P < 0.001$; ****$P < 0.0001$.

(Fig. 4C) inhibited WT-AKT1 but not T12-AKT1. The same behavior was apparent for other duplications (data not shown). The result for A-674563 is not shown because this drug had a negative impact on cell viability. Finally, it should be noted that endogenous AKT was inhibited by all tested inhibitors (i.e. NLS-mCherry and FOXO3a conditions showed a stronger activity of FOXO3a in the presence of inhibitor with respect to the dimethyl sulfoxide/DMSO condition).

In order to test another kind of inhibitor, we treated cells with GSK690693, which is a pan-AKT inhibitor that competes with ATP for binding to the ATP acceptor site in the catalytic AKT domain (39). In the presence of 10 μM of GSK690693, WT-AKT1 and all the mutated AKT1 forms tested were no longer able to repress FOXO3a (Fig. 5A). Next, we performed a western blot analysis in order to explore the phosphorylation status of AKT1 in our experiment (Fig. 5B). WT and mutated forms of AKT1 were hyperphosphorylated in the presence of GSK690693, irrespective of the presence of serum. This is consistent with previous reports showing that binding of this inhibitor to AKT1 increases phosphorylation of T308 and S473 residues, yet it effectively inhibits its kinase activity (40,41). Unfortunately, we do not have JGCT cell lines carrying abnormal AKT1 forms to test the effect of the inhibitors *in cellula* or in xenografted mice. A project to develop such cell lines is ongoing.

Taken altogether, our results suggest that the tandem duplications within AKT1 are the most likely cause of JGCT development. We also report the existence of an *AKT1* insertion in one AGCT without *FOXL2* mutation. This finding brings more questions than answers, and further analyses are required to explore the genomic and transcriptomic landscapes of such AGCTs compared with JGCTs and to more 'typical' AGCTs. Our RNA-Seq analysis uncovered transcriptomic signatures in the JGCTs and suggests that they may be mediated by a limited set of perturbed TFs.

The PI3K-AKT pathway is critical for the regulation of cell proliferation and survival. Somatic variations in *PI3K* and/or *AKT* can lead to overgrow phenotypes such as congenital lipomatous overgrowth, vascular malformations, epidermal nevi, scoliosis/skeletal and spinal syndrome (OMIM: 612 918), macrodactyly, the megalencephaly-capillary malformation syndrome (OMIM: 602 501) and proteus syndrome (OMIM: 176 920), among others (42). The wide phenotypic range observed in PIK3CA/AKT-related disorders likely defines a spectrum of mosaic overgrowth phenotypes. Thus, it is tempting to propose that JGCTs somehow belong to this spectrum. In keeping with this idea, a previous report describes two ovarian neoplasms composed of an admixture of adenosarcoma and a predominant stromal component similar to a JGCT. The authors speculate that, in both cases, the JGCT component arose from the adenosarcoma as an unusual form of sarcomatous overgrowth of sex cord elements (43). This would explain the atypical characteristic of these tumors, which were considered for years as rather 'benign' neoplasias (44).

Finally, we have explored the *in vitro* effects of several AKT inhibitors on the activity of various mutated AKT versions. Our encouraging results require *in vivo* validation, but they already provide therapeutic leads for a targeted treatment of this malignancy.

Materials and Methods

Patients

This study involves a cohort of 16 pathologically diagnosed JGCTs, occurring in girls under 15 years of age, collected between 1994 and 2014 (from the Necker-Enfants Malades Hospital, Paris and the University Hospital Montpellier tumor repositories). Twelve JGCT samples were formalin-fixed paraffin-embedded/FFPE samples (T1–T12). Four tumors were obtained as frozen samples (T13–T16). The FFPE samples of AGCTs without the C134W mutation in FOXL2 were provided by Hospital de la Santa Creu i Sant Pau, Barcelona, Spain. The control RNAs were obtained from pooled adult granulosa cells and from a normal prepubertal ovary. This study was validated by the Ethics Committees of the institutions that contributed the samples.

Nucleic acids extraction and sequencing

We isolated genomic DNA and RNA from FFPE tumors using the AllPrep DNA/RNA FFPE Kit (Qiagen), and the frozen ones were processed using standard procedures. The Sanger sequencing was performed by MWG-Biotech-AG according to their in-house procedures.

AKT1 expression constructs

The plasmids driving the expression of WT and mutated AKT1 fused to the mCherry protein were constructed by fusion PCR. Briefly, for the insertion mutations, two PCRs were performed to generate the 5′ and 3′ portions of the AKT1 coding sequence using, respectively, AKT1RED-EcoR1-F primer and the corresponding mutagenic R primer and AKT1RED-BamH1-R and AKT1-F2 primer. After purification of the PCR products, they were quantified, mixed in similar amounts and allowed to undergo eight cycles of PCR in the absence of primers, to generate the full-length mutated coding regions. Then, a final PCR reaction was performed using the EcoR1-BamHI primers. The amplified EcoR1-BamHIs were cloned (EcoR1-BamHI) into digested pDsRed vector to produce fusion proteins in frame with the mCherry. All constructs were sequenced to exclude the presence of PCR-induced mutations. The sequences of the primers used are the following:

AKT1RED-EcoR1-F: 5′ AGCTTCGAATTCGCCACCATGAGCGAC GTGGCTATTGTGAAGG 3′

AKT1-F2: 5′ GTGGACCACTGTCATCG 3′

AKT1RED-BamH1-R: 5′ ACCGGTGGATCCCG GGCCGTGCCGCT GGCCGAGTAGGAGAAC 3′

InsertT1R: 5′ CGATGACAGTGGTCCACTGCAGGCAGCGGATG ATGAAGGTGTTGGGCCGGGGCCGCTCCGTCTTCATGATGAAGGTG TTGGGCCGGGGCCGCTCC 3′

The other constructs are those described in (22).

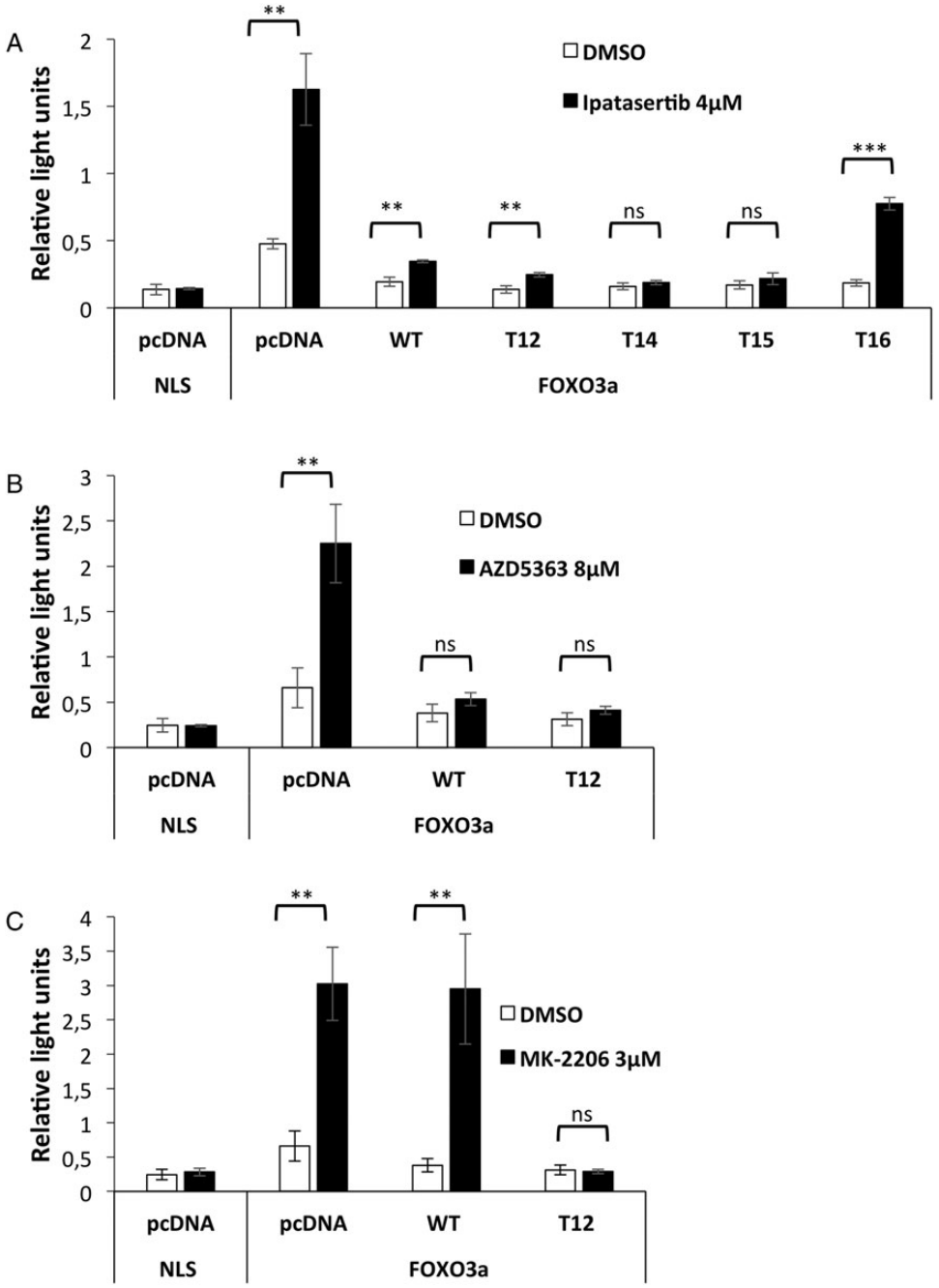

Figure 4. Effect of AKT inhibitors on the activity of WT and mutated forms (Luciferase assays). HeLa cells were co-transfected with 2X-DBE-luc and the various constructs driving the expression of WT or mutated AKT1 forms. AKT1-dependent phosphorylation of FOXO3a causes its cytoplasmic sequestration and prevents transactivation of its targets. Cells were treated for 24 h with DMSO (vehicle) or 4 µM of Ipatasertib (**A**), 6 µM of MK-2206 (**B**) and 8 µM of AZD5363 (**C**) before luciferase assay. Error bars represent the standard deviation of three replicates. The results are representative of two independent experiments. The differences between the WT and mutated AKT1 (in the absence of serum) tested using a two-sided Student's *t*-test were all highly significant (**$P < 0.01$). The mutated AKT1 variants tested were T12 c.181_228dup, p.(Gln61_Arg76dup), T14 c.202_237dup, p.(Pro68_Gln79dup); T15 c.207_230dup, p.(Arg76_Cys77insTrpProAsnThrPheIleIleArg) and T16 c.197_232dup, p.(Cys77_Leu78insGlnArgProArgProAsnThrPheIleIleArgCys).

Paired-end RNA-Seq of the four frozen tumor samples

This approach was performed by the Platform IMAGIF from the French Centre National de la Recherche Scientifique (www.imagif.cnrs.fr) on an Illumina HiSeq1000 instrument using their in-house standard protocols. On average, 60 million sequence reads per sample were mapped for mutation detection purposes, allowing only two mismatches between the read and the target. Details on the analysis are provided in the Supplementary Material.

RNA-Seq differential expression analysis

We used the reads mapped for mutation detection purposes in the four JGCTs and the two control samples. This strategy

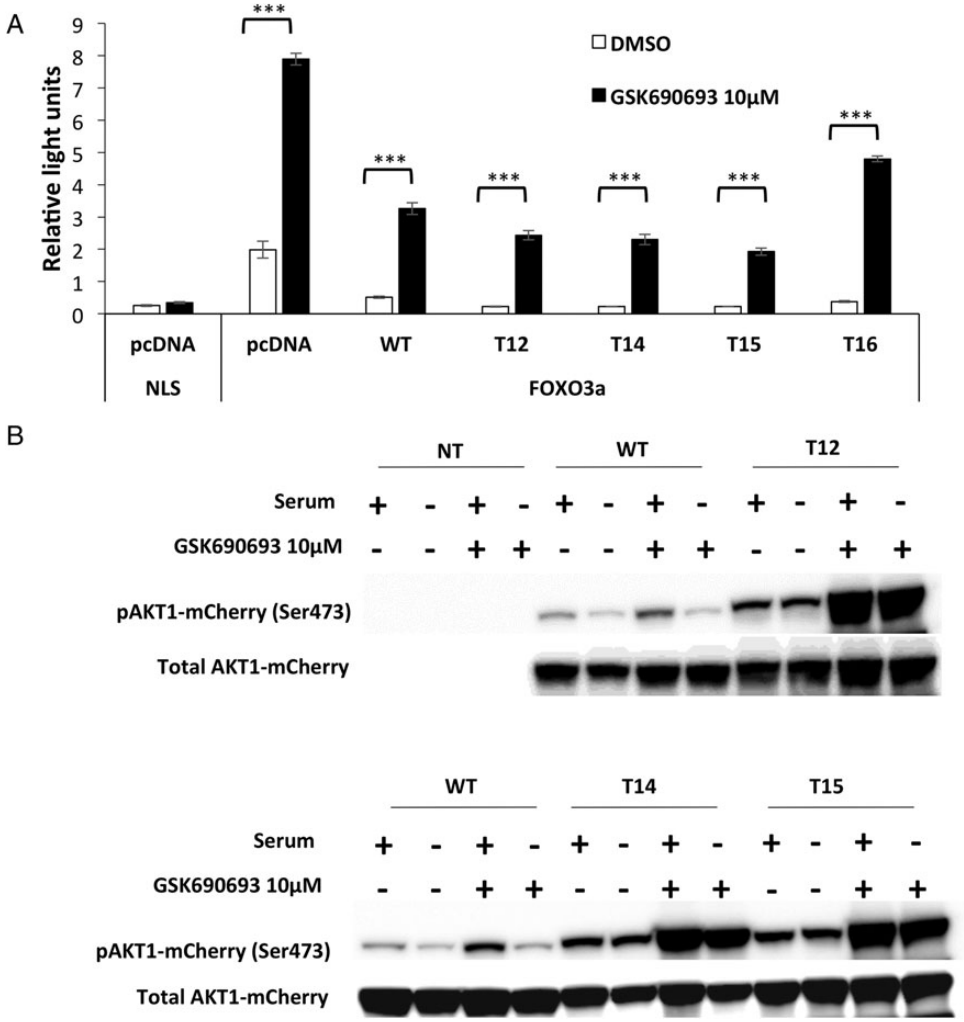

Figure 5. AKT1 activity and phosphorylation status in the presence of GSK690693. (**A**) HeLa cells were treated 24 h with DMSO (vehicle) or 10 µM of GSK690693 before luciferase assay (as described in Fig. 4). Error bars represent the standard deviation of three replicates. The results are representative of two independent experiments. The differences between the WT and mutated AKT1 (in the absence or the presence of serum) tested using a two-sided Student's *t*-test were all highly significant (***$P < 0.001$). (**B**) Western blot analysis of the phosphorylation levels of several AKT1 variants (WT, T12, T13 and T14 proteins). NT: not transfected. For each variant, four conditions are tested: with and without serum with DMSO (vehicle) or 10 µM of GSK690693.

reduced the number of reads per sample treated but increased the specificity of the analysis (i.e. virtually no possible confusion among paralogs, etc.). The analysis was performed using the Tuxedo suite on the Galaxy server (45). Specifically, the transcriptome was assembled separately for each sample with Cufflinks, using the hg19 UCSC reference transcriptome as a guide. The six assembled transcriptomes were merged using Cuffmerge. Then, the two control conditions were compared with the test conditions (four tumors) using Cuffdiff. The set of 460 DE genes were analyzed for gene set enrichment using the Enrichr server (http://amp.pharm.mssm.edu/Enrichr/enrich) (46). The Bonferroni correction was applied to all *P*-values associated with enrichments to select only the highly significant ones. The Gene Set Enrichment Analysis for ChIP targets was further explored by compiling the known targets within the 460 DE genes for all TF with statistically over-represented ChIP peaks according to the Enrichr analysis. Therefore, we constructed a table containing one column for each of the 155 'ChIP-TFs', with 460 rows representing the DE genes, and the absence/presence of a ChIP peak encoded in a binary way (0 or 1). This matrix was first simplified by removing 40 DE genes not significantly bound by any TF. It was further refined by calculating Pearson's correlation coefficient between the vectors representing the TFs (i.e. columns), and keeping only the TFs significantly correlated with at least another TF (for $n = 420$, the threshold used for R was 0.22, to obtain a significant Bonferroni-corrected *P*-value). The same procedure was applied to rows, in order to keep only DE genes significantly correlated to at least one other gene (in this case, for $n = 155$, the threshold used for R was 0.38, to obtain a significant Bonferroni-corrected *P*-value). Finally, we removed 11 TFs neither expressed in our controls nor in JGCTs, according to our RNA-Seq data. The resulting matrix contained 332 genes and 105 ChIP-TFs. Hierarchical clustering of the latter matrix was performed with MeV 4.8 (http://www.tm4.org/mev.html) (47), using Pearson's correlation as a measure of similarity and average linkage. In parallel, we explored the enrichment of the 460 DE genes for genes whose expression changes in mouse or cellular models of *l*oss or *g*ain of *f*unction for specific TFs ('logof-TFs'). The over-representation of AKT1 and GSK3β targets in the 45 identified logof-TFs was assessed using Enrichr. For all the lists obtained above, the significance of relevant overlaps was assessed using the L2N Overlap tool (http://amp.pharm.mssm.edu/l2n/) (48).

The direct protein–protein interactions were retrieved using the Expand tool in L2N with PathLength 1 and sensitivity ranging from 5 to 45, and the network was constructed using Cytoscape 3.2.1 (http://www.cytoscape.org) (49).

Cell culture, luciferase assays and western blot

The HeLa cell lines were used for functional studies with AKT inhibitors. They were grown in Dulbecco's modified Eagle's medium-F12 medium (Gibco®, Life Technologies, Grand Island, NY, USA), supplemented with 10% fetal bovine serum (FBS) and 1% penicillin/streptomycin (Invitrogen-Gibco, Life Technologies).

Dual-Luciferase Reporter Assays (Promega, Madison, WI, USA) involved the reporter promoter 2XDBE-luc, which contains two copies of the FOXO response element (DAF-16 family member-binding element or DBE) upstream of a minimal promoter driving the expression of the firefly luciferase gene (50). Each experiment was performed in three replicates in 96-well plates. Cells were seeded 16 h before transfection to be at confluence at the time of transfection and transfected with 280 ng of total DNA per well [2X DBE-luc, AKT1 vector, FOXO3a (Addgen n° 1787) or NLS-control vector and renilla luciferase vector] using the calcium phosphate method and rinsed 24 h after transfection. At this point, cells were treated with inhibitor or DMSO. The AKT1 inhibitors used were A-674563, AZD5363, Ipatasertib, GSK690693 and MK-2206 2HCl (SelleckChem, references S2670, S8019, S2808, S1113 and S1078, respectively). All compounds are pan-Akt inhibitors except A-674563, which targets only AKT1. Inhibitors were dissolved in DMSO and were used in cell culture at the following concentrations: A-674563 (500 nM), AZD5363 (8 µM), Ipatasertib (4 µM), GSK690693 (10 µM) and MK-2206 2HCl (6 µM). Forty-eight hours after transfection, cells were washed with phosphate-buffered saline before lysis, and luciferase measurements were performed with a TriStar LB 941 luminometer (Berthold Technologies, Bad Wildbad, Germany). To monitor transfection efficiency, a Renilla luciferase vector (pRL-RSV, Promega) was co-transfected. Activity is expressed as relative luciferase units (RLU, i.e. the ratio of the firefly luciferase activity over the Renilla luciferase activity). Statistical significance was estimated by Student's *t*-tests. Error bars represent the standard deviation between replicates.

For western blot studies, HeLa cells were transfected with the constructs driving the expression of WT or mutated AKT1 forms. One day after transfection, cells were rinsed, serum-starved or not and treated with 10 µM of GSK690693 or DMSO for 24 h before lysis. Electrophoresis and western blot were performed as previously described (21,33).

Supplementary Material

Supplementary Material is available at *HMG* Online.

Conflict of Interest statement. None declared.

Funding

This work was supported by Groupement des Entreprises Françaises dans la Lutte contre le Cancer (GEFLUC), the Centre National de la Recherche Scientifique (CNRS) and the Université Paris Diderot and the Agence Nationale pour la Recherche.

References

1. Young, R.H. and Scully, R.E. (1992) Endocrine tumors of the ovary. *Curr. Top. Pathol. Ergeb. Pathol.*, **85**, 113–164.
2. Segal, R., DePetrillo, A.D. and Thomas, G. (1995) Clinical review of adult granulosa cell tumors of the ovary. *Gynecol. Oncol.*, **56**, 338–344.
3. Schumer, S.T. and Cannistra, S.A. (2003) Granulosa cell tumor of the ovary. *J. Clin. Oncol. Off. J. Am. Soc. Clin. Oncol.*, **21**, 1180–1189.
4. Vassal, G., Flamant, F., Caillaud, J.M., Demeocq, F., Nihoul-Fekete, C. and Lemerle, J. (1988) Juvenile granulosa cell tumor of the ovary in children: a clinical study of 15 cases. *J. Clin. Oncol. Off. J. Am. Soc. Clin. Oncol.*, **6**, 990–995.
5. Young, R.H., Dickersin, G.R. and Scully, R.E. (1984) Juvenile granulosa cell tumor of the ovary. A clinicopathological analysis of 125 cases. *Am. J. Surg. Pathol.*, **8**, 575–596.
6. Calaminus, G., Wessalowski, R., Harms, D. and Göbel, U. (1997) Juvenile granulosa cell tumors of the ovary in children and adolescents: results from 33 patients registered in a prospective cooperative study. *Gynecol. Oncol.*, **65**, 447–452.
7. Zaloudek, C. and Norris, H.J. (1982) Granulosa tumors of the ovary in children: a clinical and pathologic study of 32 cases. *Am. J. Surg. Pathol.*, **6**, 503–512.
8. Biscotti, C.V. and Hart, W.R. (1989) Juvenile granulosa cell tumors of the ovary. *Arch. Pathol. Lab. Med.*, **113**, 40–46.
9. Sivasankaran, S., Itam, P., Ayensu-Coker, L., Sanchez, J., Egler, R.A., Anderson, M.L., Brandt, M.L. and Dietrich, J.E. (2009) Juvenile granulosa cell ovarian tumor: a case report and review of literature. *J. Pediatr. Adolesc. Gynecol.*, **22**, e114–e117.
10. Merras-Salmio, L., Vettenranta, K., Möttönen, M. and Heikinheimo, M. (2002) Ovarian granulosa cell tumors in childhood. *Pediatr. Hematol. Oncol.*, **19**, 145–156.
11. Schrader, K.A., Gorbatcheva, B., Senz, J., Heravi-Moussavi, A., Melnyk, N., Salamanca, C., Maines-Bandiera, S., Cooke, S.L., Leung, P., Brenton, J.D. *et al.* (2009) The specificity of the FOXL2 c.402C>G somatic mutation: a survey of solid tumors. *PloS One*, **4**, e7988.
12. Jamieson, S., Butzow, R., Andersson, N., Alexiadis, M., Unkila-Kallio, L., Heikinheimo, M., Fuller, P.J. and Anttonen, M. (2010) The FOXL2 C134W mutation is characteristic of adult granulosa cell tumors of the ovary. *Mod. Pathol. Off. J. U. S. Can. Acad. Pathol. Inc*, **23**, 1477–1485.
13. Benayoun, B.A., Caburet, S., Dipietromaria, A., Georges, A., D'Haene, B., Pandaranayaka, P.J.E., L'Hôte, D., Todeschini, A.-L., Krishnaswamy, S., Fellous, M. *et al.* (2010) Functional exploration of the adult ovarian granulosa cell tumor-associated somatic FOXL2 mutation p.Cys134Trp (c.402C>G). *PloS One*, **5**, e8789.
14. Rosario, R., Araki, H., Print, C.G. and Shelling, A.N. (2012) The transcriptional targets of mutant FOXL2 in granulosa cell tumours. *PloS One*, **7**, e46270.
15. Kalfa, N., Philibert, P., Patte, C., Ecochard, A., Duvillard, P., Baldet, P., Jaubert, F., Fellous, M. and Sultan, C. (2007) Extinction of FOXL2 expression in aggressive ovarian granulosa cell tumors in children. *Fertil. Steril.*, **87**, 896–901.
16. Kalfa, N., Ecochard, A., Patte, C., Duvillard, P., Audran, F., Pienkowski, C., Thibaud, E., Brauner, R., Lecointre, C., Plantaz, D. *et al.* (2006) Activating mutations of the stimulatory g protein in juvenile ovarian granulosa cell tumors: a new prognostic factor? *J. Clin. Endocrinol. Metab.*, **91**, 1842–1847.
17. Landis, C.A., Masters, S.B., Spada, A., Pace, A.M., Bourne, H.R. and Vallar, L. (1989) GTPase inhibiting mutations activate the alpha chain of Gs and stimulate adenylyl cyclase in human pituitary tumours. *Nature*, **340**, 692–696.
18. Chien, J., Wong, E., Nikes, E., Noble, M.J., Pantazis, C.G. and Shah, G.V. (1999) Constitutive activation of stimulatory guanine nucleotide binding protein (G(S)alphaQL)-mediated signaling increases invasiveness and tumorigenicity of PC-3M prostate cancer cells. *Oncogene*, **18**, 3376–3382.

19. Régnauld, K., Nguyen, Q.-D., Vakaet, L., Bruyneel, E., Launay, J.-M., Endo, T., Mareel, M., Gespach, C. and Emami, S. (2002) G-protein alpha(olf) subunit promotes cellular invasion, survival, and neuroendocrine differentiation in digestive and urogenital epithelial cells. *Oncogene*, **21**, 4020–4031.
20. Hunzicker-Dunn, M.E., Lopez-Biladeau, B., Law, N.C., Fiedler, S.E., Carr, D.W. and Maizels, E.T. (2012) PKA and GAB2 play central roles in the FSH signaling pathway to PI3 K and AKT in ovarian granulosa cells. *Proc. Natl. Acad. Sci. USA*, **109**, E2979–E2988.
21. Baumgarten, S.C., Convissar, S.M., Fierro, M.A., Winston, N.J., Scoccia, B. and Stocco, C. (2014) IGF1R signaling is necessary for FSH-induced activation of AKT and differentiation of human cumulus granulosa cells. *J. Clin. Endocrinol. Metab.*, **99**, 2995–3004.
22. Bessière, L., Todeschini, A.L., Auguste, A., Sarnacki, S., Flatters, D., Legois, B., Sultan, C., Kalfa, N., Galmiche, L. and Veitia, R. (2015) A hot-spot of in-frame duplications activates the oncoprotein AKT1 in juvenile granulosa cell tumors. *EBioMedicine*, **2**, 421–431.
23. Franke, T.F., Kaplan, D.R., Cantley, L.C. and Toker, A. (1997) Direct regulation of the Akt proto-oncogene product by phosphatidylinositol-3,4-bisphosphate. *Science*, **275**, 665–668.
24. Warfel, N.A., Niederst, M. and Newton, A.C. (2011) Disruption of the interface between the pleckstrin homology (PH) and kinase domains of Akt protein is sufficient for hydrophobic motif site phosphorylation in the absence of mTORC2. *J. Biol. Chem.*, **286**, 39122–39129.
25. Carpten, J.D., Faber, A.L., Horn, C., Donoho, G.P., Briggs, S.L., Robbins, C.M., Hostetter, G., Boguslawski, S., Moses, T.Y., Savage, S. *et al.* (2007) A transforming mutation in the pleckstrin homology domain of AKT1 in cancer. *Nature*, **448**, 439–444.
26. Yi, K.H., Axtmayer, J., Gustin, J.P., Rajpurohit, A. and Lauring, J. (2013) Functional analysis of non-hotspot AKT1 mutants found in human breast cancers identifies novel driver mutations: implications for personalized medicine. *Oncotarget*, **4**, 29–34.
27. Calnan, D.R. and Brunet, A. (2008) The FoxO code. *Oncogene*, **27**, 2276–2288.
28. Robinson, J.T., Thorvaldsdóttir, H., Winckler, W., Guttman, M., Lander, E.S., Getz, G. and Mesirov, J.P. (2011) Integrative genomics viewer. *Nat. Biotechnol.*, **29**, 24–26.
29. Benayoun, B.A., Anttonen, M., L'Hôte, D., Bailly-Bechet, M., Andersson, N., Heikinheimo, M. and Veitia, R.A. (2013) Adult ovarian granulosa cell tumor transcriptomics: prevalence of FOXL2 target genes misregulation gives insights into the pathogenic mechanism of the p.Cys134Trp somatic mutation. *Oncogene*, **32**, 2739–2746.
30. Sistigu, A., Yamazaki, T., Vacchelli, E., Chaba, K., Enot, D.P., Adam, J., Vitale, I., Goubar, A., Baracco, E.E., Remédios, C. *et al.* (2014) Cancer cell-autonomous contribution of type I interferon signaling to the efficacy of chemotherapy. *Nat. Med.*, **20**, 1301–1309.
31. Kaur, S., Sassano, A., Dolniak, B., Joshi, S., Majchrzak-Kita, B., Baker, D.P., Hay, N., Fish, E.N. and Platanias, L.C. (2008) Role of the Akt pathway in mRNA translation of interferon-stimulated genes. *Proc. Natl. Acad. Sci. USA*, **105**, 4808–4813.
32. Cheon, H., Borden, E.C. and Stark, G.R. (2014) Interferons and their stimulated genes in the tumor microenvironment. *Semin. Oncol.*, **41**, 156–173.
33. Liu, Z., Ren, Y.A., Pangas, S.A., Adams, J., Zhou, W., Castrillon, D.H., Wilhelm, D. and Richards, J.S. (2015) FOXO1/3 and PTEN depletion in granulosa cells promotes ovarian granulosa cell tumor development. *Mol. Endocrinol. Baltim. Md.*, **29**, 1006–1024.
34. Li, G., Margueron, R., Ku, M., Chambon, P., Bernstein, B.E. and Reinberg, D. (2010) Jarid2 and PRC2, partners in regulating gene expression. *Genes Dev.*, **24**, 368–380.
35. Biggin, M.D. (2011) Animal transcription networks as highly connected, quantitative continua. *Dev. Cell*, **21**, 611–626.
36. MacArthur, S., Li, X.-Y., Li, J., Brown, J.B., Chu, H.C., Zeng, L., Grondona, B.P., Hechmer, A., Simirenko, L., Keränen, S.V.E. *et al.* (2009) Developmental roles of 21 Drosophila transcription factors are determined by quantitative differences in binding to an overlapping set of thousands of genomic regions. *Genome Biol.*, **10**, R80.
37. Don, A.S.A. and Zheng, X.F.S. (2011) Recent clinical trials of mTOR-targeted cancer therapies. *Rev. Recent Clin. Trials*, **6**, 24–35.
38. Pal, S.K., Reckamp, K., Yu, H. and Figlin, R.A. (2010) Akt inhibitors in clinical development for the treatment of cancer. *Expert Opin. Investig. Drugs*, **19**, 1355–1366.
39. Levy, D.S., Kahana, J.A. and Kumar, R. (2009) AKT inhibitor, GSK690693, induces growth inhibition and apoptosis in acute lymphoblastic leukemia cell lines. *Blood*, **113**, 1723–1729.
40. Okuzumi, T., Fiedler, D., Zhang, C., Gray, D.C., Aizenstein, B., Hoffman, R. and Shokat, K.M. (2009) Inhibitor hijacking of Akt activation. *Nat. Chem. Biol.*, **5**, 484–493.
41. Rhodes, N., Heerding, D.A., Duckett, D.R., Eberwein, D.J., Knick, V.B., Lansing, T.J., McConnell, R.T., Gilmer, T.M., Zhang, S.-Y., Robell, K. *et al.* (2008) Characterization of an Akt kinase inhibitor with potent pharmacodynamic and antitumor activity. *Cancer Res.*, **68**, 2366–2374.
42. Keppler-Noreuil, K.M., Sapp, J.C., Lindhurst, M.J., Parker, V.E. R., Blumhorst, C., Darling, T., Tosi, L.L., Huson, S.M., Whitehouse, R.W., Jakkula, E. *et al.* (2014) Clinical delineation and natural history of the PIK3CA-related overgrowth spectrum. *Am. J. Med. Genet. A.*, **164A**, 1713–1733.
43. Carleton, C., Houghton, O.P. and McCluggage, W.G. (2015) Juvenile granulosa cell tumor arising in ovarian adenosarcoma: an unusual form of sarcomatous overgrowth. *Hum. Pathol.*, **46**, 614–619.
44. Kalfa, N. and Sultan, C. (2009) Juvenile ovarian granulosa cell tumor: a benign or malignant condition? *Gynecol. Endocrinol. Off. J. Int. Soc. Gynecol. Endocrinol.*, **25**, 299–302.
45. Goecks, J., Nekrutenko, A. and Taylor, J. and Galaxy Team. (2010) Galaxy: a comprehensive approach for supporting accessible, reproducible, and transparent computational research in the life sciences. *Genome Biol.*, **11**, R86.
46. Chen, E.Y., Tan, C.M., Kou, Y., Duan, Q., Wang, Z., Meirelles, G. V., Clark, N.R. and Ma'ayan, A. (2013) Enrichr: interactive and collaborative HTML5 gene list enrichment analysis tool. *BMC Bioinformatics*, **14**, 128.
47. Saeed, A.I., Sharov, V., White, J., Li, J., Liang, W., Bhagabati, N., Braisted, J., Klapa, M., Currier, T., Thiagarajan, M. *et al.* (2003) TM4: a free, open-source system for microarray data management and analysis. *BioTechniques*, **34**, 374–378.
48. Lachmann, A. and Ma'ayan, A. (2010) Lists2Networks: integrated analysis of gene/protein lists. *BMC Bioinformatics*, **11**, 87.
49. Shannon, P., Markiel, A., Ozier, O., Baliga, N.S., Wang, J.T., Ramage, D., Amin, N., Schwikowski, B. and Ideker, T. (2003) Cytoscape: a software environment for integrated models of biomolecular interaction networks. *Genome Res.*, **13**, 2498–2504.
50. Furuyama, T., Nakazawa, T., Nakano, I. and Mori, N. (2000) Identification of the differential distribution patterns of mRNAs and consensus binding sequences for mouse DAF-16 homologues. *Biochem. J.*, **349**, 629–634.